JOURNAL OF MATERIALS SCIENCE 22 (1987) 715–721

Europium precipitates in monocrystalline NaCl

Part 1 *General features of as-grown state*

M. SUSZYŃSKA, H. OPYRCHAŁ, M. CZAPELSKI
Institute of Low Temperature and Structure Research, Polish Academy of Sciences, Wrocław, Poland

M. MANFREDI
Dipartimento di Fisica, Universita Degli Studi di Parma, Parma, Italy

As-grown and well aged at room temperature NaCl crystals doped with divalent europium were systematically studied by using optical, dielectrical and mechanical methods. It has been found that at room temperature the optical absorption spectrum of these crystals is strongly concentration-dependent. The role of the dopant concentration has been also evidenced by photoluminescence (taken at liquid nitrogen temperature) thermally stimulated depolarization current techniques and the mechanical response of the as-grown crystals. The experimental results obtained have been explained by assuming that the increase of the dopant concentration is accompanied by structural changes of the Eu^{2+}-related precipitates from impurity–vacancy dipoles and small aggregates to orthorhombic $EuCl_2$ of $PbCl_2$-type.

1. Introduction

Precipitates of the second phase particles in alkali halide crystals doped with divalent cations take different structural forms which in the case of heavily doped crystals can be detected by precise X-ray diffraction and electron microscopy methods. In the case of slightly doped crystals some relevant information can be obtained by studying the changes of structure-sensitive properties induced by various external agents. Europium-doped NaCl crystals are of the particular interest here because the information obtained in a more or less indirect way can be directly compared with the microstructural data [1, 2].

The present paper opens a series of reports dealing with the precipitation phenomena in europium-doped NaCl crystals, whereby

Part 1 presents the basic characteristics of as-grown (AG) crystals, and

Part 2 deals with the precipitation phenomenon provoked by the annealing of solution treated (ST) samples.

Systematic studies of the optical properties have been completed by data obtained from measurements of dielectrical and mechanical characteristics.

The sensitivity of the optical properties of NaCl: Eu^{2+} crystals to the dispersion state of the dopant has been the subject of previous investigations [3–5]. However, as will be shown in the present paper, the available information is far from complete.

2. Experimental details

The crystals were grown in our laboratory by the modified Bridgman method at least two years ago. The pretreatment of the molten NaCl: Eu_2O_3 mixture with gaseous $COCl_2$ assures the diminution of oxygen-containing impurities below the optically detectable limit [6]. The dopant enters the crystal lattice exclusively in the form of divalent ions. A high density (approximately equal to $2 \times 10^6 cm^{-2}$) of grown-in dislocations in the form of strongly fastened dislocation network may be regarded as a substantial disadvantage of the growth procedure.

The amount of divalent europium (in the samples) is given by the value of the absorption coefficient characteristic of the europium-related high-energy absorption band, $\alpha(e_g)$. Unfortunately, the correlation factor between $\alpha(e_g)$ and the europium concentration found for the slightly doped ST crystals [7, 8] is inapplicable for heavily doped ones as the ratio of $\alpha(e_g)$ for the AG and ST states display different numerical values. The value of $\alpha(e_g)$ characteristic of the used AG samples covers the range between 1 and $100\,cm^{-1}$.

The optical as well as dielectric characteristics were measured for thin crystal slabs, of approximate dimensions 0.3 mm × 4 mm × 10 mm, cut from larger crystal blocks with a nearly identical content for the dopant. Optical absorption spectra were taken at room temperature (RT) with a Specord (Zeiss) UV–visible spectrophotometer in the spectral range between 200 and 450 nm. The emission spectra and the luminescence decay time, measured as function of the emitted light (λ_{em} = 400 to 500 nm), were taken at liquid nitrogen temperature (LNT) and RT by using the arrangement described in [4]. The emission data were obtained for an excitation wavelength selected within the high-energy (e_g) absorption band.

Thermally stimulated depolarization current (ITC) technique [9] was mainly exploited for the detection of impurity–vacancy (I–V) dipoles. For some samples the entire ITC spectrum was measured (in an extended temperature range) in order to detect the induced polarization phenomena related to the presence of

0022–2461/87 $03.00 + .12

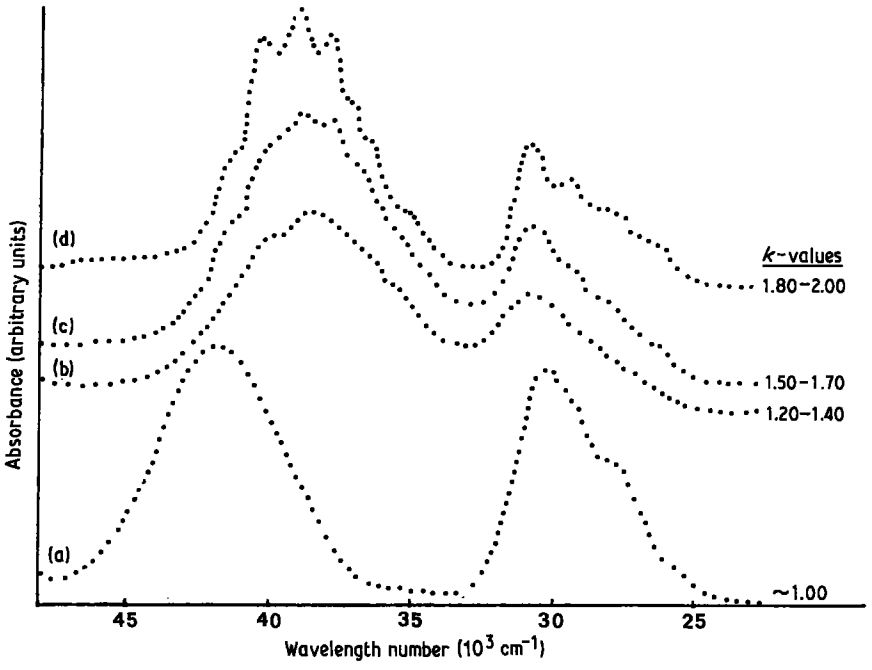

Figure 1 Optical absorption spectra (taken at room temperature) characteristic of four groups of AG NaCl:Eu^{2+} crystals: (a) $\alpha(e_g) < 11\,cm^{-1}$, (b) $\alpha(e_g) = 11.5$ to $25\,cm^{-1}$, (c) $\alpha(e_g) = 28.9$ to $43.6\,cm^{-1}$, (d) $\alpha(e_g) > 45\,cm^{-1}$.

some precipitate particles segregated near the dislocation lines [10, 11].

The parallelepiped-shaped samples, of approximate dimensions 3 mm × 3 mm × 9 mm, were used for mechanical testing performed in the Instron machine (model 1112) (High Wycombe, UK). The compression load was applied in the [0 0 1] direction, and the strain rate ($\dot{\varepsilon}$) realized was equal to $3 \times 10^{-4}\,sec^{-1}$. From the dependence of the shape of the stress–strain curves, the yield stress value (σ_0) was determined either from 0.2% plastic strain or as the value of σ which corresponds to the intersection of the linear elastic and easy glide range. The work hardening rate (θ) was determined for the initial deformation range.

Although the data mainly concerned the behaviour of AG crystals, some information is also given for ST crystals. The solution treatment (ST) procedure comprised the annealing at 873 K for 30 min and quenching on a metal block at RT. As has been previously evidenced [8] the realized cooling rate is not rapid enough to prevent some aggregation in crystals with $\alpha(e_g)$ as low as $\sim 21\,cm^{-1}$. More severe quenching (e.g. by immersion in liquid nitrogen) resulted in intense cracking of the samples.

3. Results and discussion

3.1. Optical characteristics

3.1.1. Absorption

It is well established that the absorption spectrum of the europium-doped alkali halides, including NaCl, consists of two broad bands located in the UV spectral range, e.g. [3, 12]. The origin of these bands is related to the allowed electric dipole transitions, $4f^7$, to the e_g and t_{2g} states of the excited $4f^6 5d$ configuration, whereby the t_{2g} states are lower in energy than the e_g ones [12].

Fig. 1 presents four types of the europium-related optical absorption spectra characteristic for four ranges of the dopant concentration, given by the value of $\alpha(e_g)$ for the AG state. Each concentration range is represented by one spectrum for which the characteristic value of $k = \alpha(e_g)/\alpha(t_{2g})$ is given.

The optical behaviour of crystals also differs with regard to the effect of the solution treatment. In contrast to $\alpha(t_{2g})$ which is always larger for the ST state than for the AG state the behaviour of $\alpha(e_g)$ under the solution treatment conditions is "concentration dependent". Three types of behaviour are characteristic of crystals with $\alpha(e_g) \gtrsim 10\,cm^{-1}$:

1. for the B-type spectrum: $\alpha(e_g)[ST] > \alpha(e_g)[AG]$
2. for the C-type spectrum: the ST treatment does not practically change the value of $\alpha(e_g)$, and
3. for the D-type spectrum: $\alpha(e_g)[ST] < \alpha(e_g)[AG]$.

The A-type spectrum, typical of crystals with the smallest value of $\alpha(e_g)$, is practically independent of the thermal history of the sample, and corresponds to the spectrum characteristic of all ST samples.

The fundamental role of the "dopant concentration" has also been evidenced by the measurements performed for freshly grown crystals nominally doped with a large amount of the admixture. Although these crystals were not aged at RT, the spectrum characteristic of the so called dirty end of the ingots is usually of the C- or D-type.

Based on these results it is assumed (as a working hypothesis) that the absorption spectra are characteristic of various forms of the europium-related precipitates. Although there is no direct evidence that the distinguished spectra correspond to single, well defined precipitate forms, it seems reasonable to expect that a given type of interaction (with all the consequences of the optical transitions) should dominate in crystals belonging to the same "concentration group".

3.1.2. Emission

In order to complete the optical characteristics, the

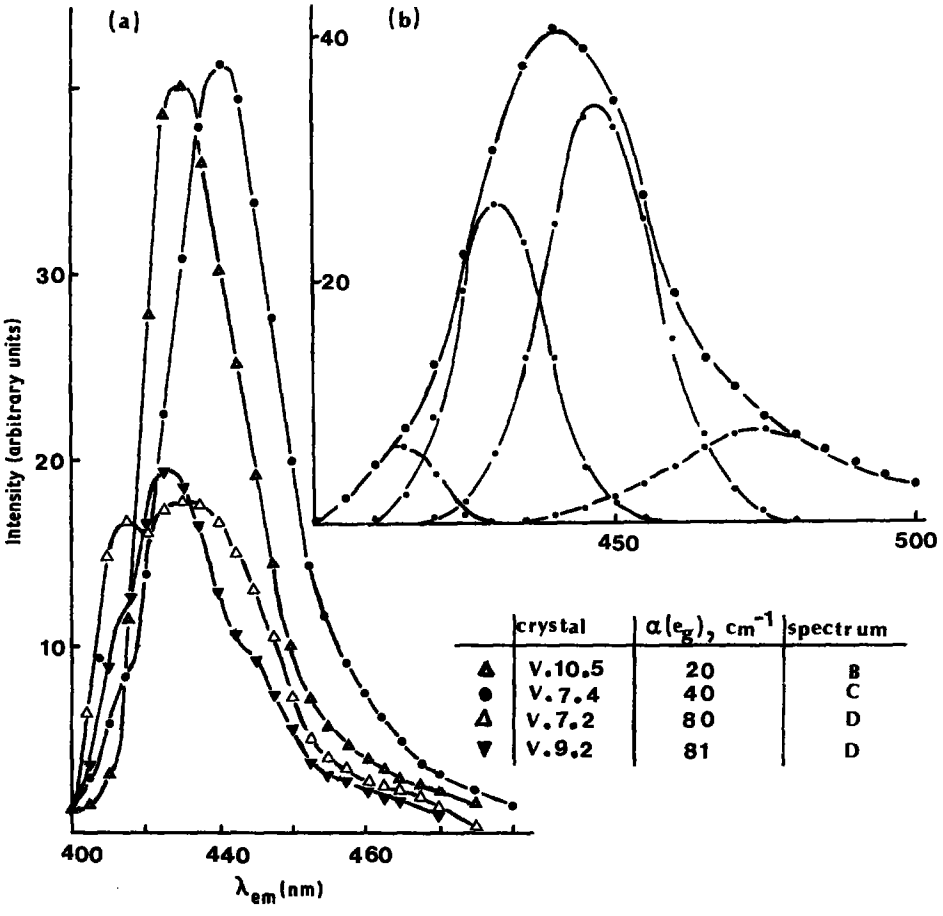

Figure 2 (a) Emission spectra of some AG NaCl:Eu^{2+} crystals taken at LNT; excitation wavelength: 260 nm, (b) Decomposition of the spectrum for the V.7.4 crystal.

AG crystals with $\alpha(e_g) \geqslant 20\,cm^{-1}$ have been excited at 260 nm, and both the emission spectrum and the luminescence time decay curve have been measured at LNT and RT.

Fig. 2 shows some examples of the emission spectra. It is clearly apparent that the degree of complexity of these spectra depends upon $\alpha(e_g)$. In general, four contributions peaking at about 415, 427, 445 and 480 nm have been detected, whereby:

the 415 nm component appears only for the most heavily doped crystals (D-type absorption spectrum),

the 427 nm component is present in all cases, although it is the most intensive one for samples with the B-type absorption spectrum,

the 445 nm component is typical of crystals with the C-type spectrum, and

the tail of the low-energy side of the emission spectrum, with slight maximum at about 480 nm, was registered for all samples studied.

The method of numerical analysis used in the resolution of the complex emission spectra was based on the non-linear least square fitting by assuming the Gaussian shape of the components. In all cases strong luminescence quenching has been observed for the AG crystals, whereas the strongest effect occurs for crystals with $\alpha(e_g) \gtrsim 40\,cm^{-1}$. Moreover, the effect of thermal quenching is also typical of this crystal system; on average, the emission intensity at RT amounts to 71% of the value registered at LNT.

It has been evidenced previously [3] that the 410 nm component (measured at RT) relates with the presence of Eu^{2+} ions in the form of the orthorhombic $EuCl_2$ phase. This could correspond to the mentioned 415 nm component, detected at LNT. From among the remaining components the 427 nm one can also be ascribed to a more or less definite dispersion form of europium. Taking into account that the ST spectrum consists of a narrow 427 nm band, e.g. [4] this component in the AG spectrum should correspond at least to the presence of I–V dipoles and small dipole aggregates formed during the cooling period from 873 K. However, as will be shown in the forthcoming Section, the ITC spectrum of AG crystals exhibits the presence of isolated dipoles for crystals with $\alpha(e_g) \lesssim 20\,cm^{-1}$ only. Hence, the 427 nm component should also be characteristic of some precipitates which emit at the same energy value. In principle, this could be the Na_2EuCl_4 particles considered as an ensemble of I–V dipoles, see [1] and Section 4. The origin of the 445 nm component has been tentatively ascribed to the presence of europium in the CaF_2-type form of $EuCl_2$ phase [1]. In order to check this hypothesis, further experiments are necessary.

3.1.3. Decay kinetics of the excited state

The complex character of the emission phenomena is also evident from the time-dependence of the luminescence decay. Fig. 3 presents two sets of data characteristic of crystals with the B-type (Fig. 3a), and C- as well as D-types (Fig. 3b) of absorption spectrum. Some further differences in the crystal behaviour have

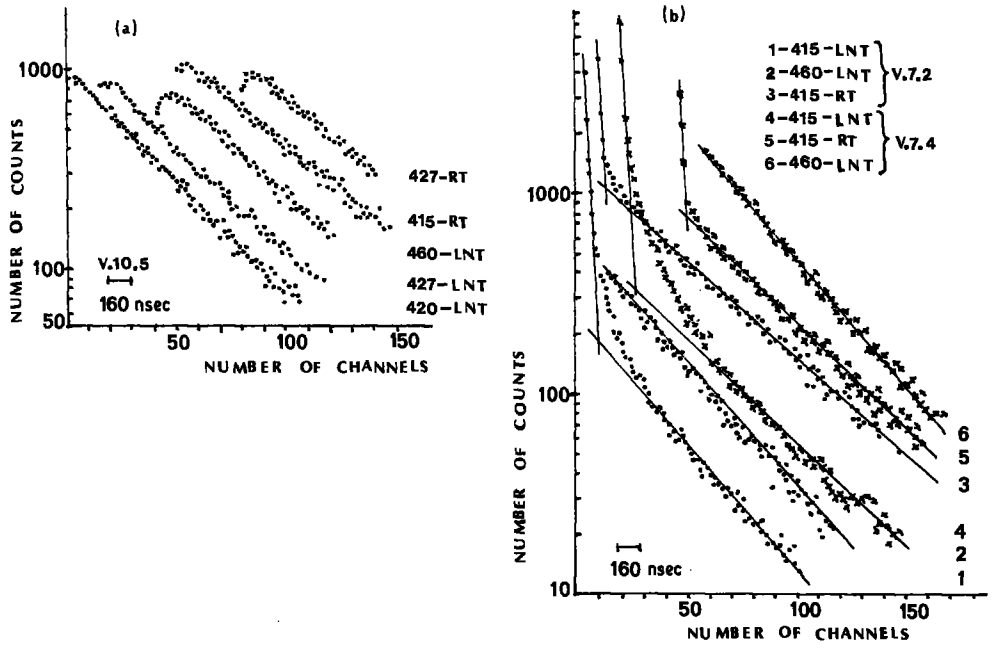

Figure 3 Semilogarithmic plot of luminescence decay-time curves for (a) V.10.5 and (b) V.7.4 as well as V.7.2 samples. The effects of both the testing temperature (T_{test}) and the emission wavelengths (λ_{em}) are exemplified.

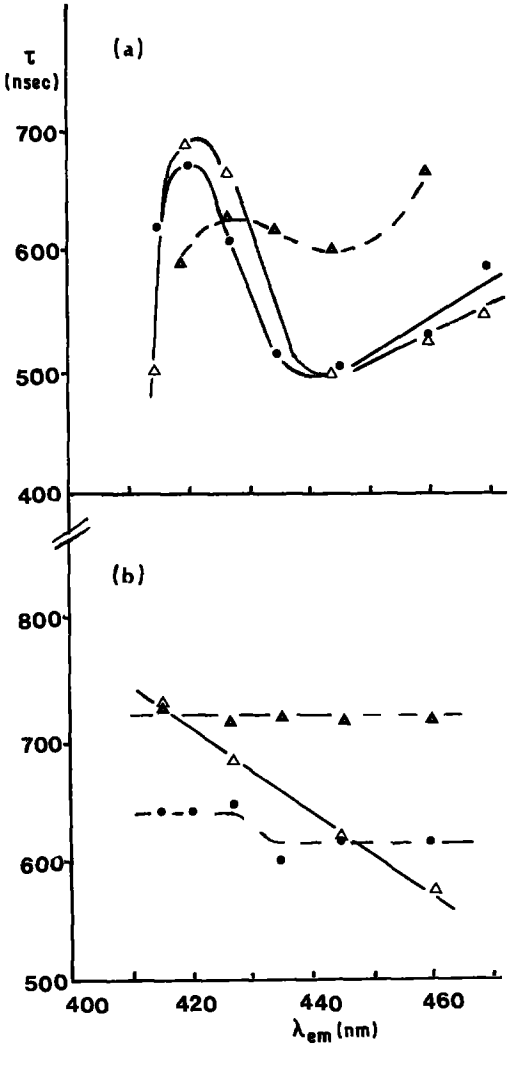

Figure 4 Luminescence decay times measured at (a) LNT and (b) RT as a function of λ_{em} for (▲) V.10.5, (●) V.7.4 and (△) V.7.2 samples.

been ascertained on the basis of lifetime (τ) values characteristic of the late stage of the luminescence decay. Fig. 4 shows the $\tau(\lambda_{em})$-dependences, where τ is defined as the "1/e-decay time", i.e. the time interval after which the luminescence has decreased by a factor of "e" from its initial value.

The most significant features to be inferred from the above results are as follows:

For slightly doped crystals practically the entire luminescence decay curve can be described by an exponential law with a unique time decay constant nearly independent of λ_{em}. The lifetime value amounts on average to 615 nsec at LNT, which is significantly smaller than the radiative lifetime value (τ_0) for ST samples of similar composition: $\tau_0 = 1000$ and 1100 nsec at 80 [4] and 15 K [5], respectively. Because of some formal similarities of the entire luminescence decay curve typical of these crystals with that detected by Heber for the N_2 line decay curve in ruby [13], it is supposed that the microscopic process responsible for this behaviour relates to the excitation energy transfer between isolated I–V dipoles and planar dimers which form the Na_2EuCl_4 particles present in these crystals.

Although the luminescence decay curve of the solution treated crystals is always exponential in the entire time scale measured, the lifetime value obtained is strongly dependent upon the cooling procedure. For instance, the value of τ obtained for the ST V.7.II ($\alpha(e_g) \simeq 80\,cm^{-1}$) sample amounts to 860 nsec at 80 K which is distinctly smaller than the τ_0 characteristic of isolated I–V dipoles present in the slightly doped ST samples [4, 5]. The lower τ value is in agreement with the finding that the solution treatment does not prevent the formation of small aggregates during the period of cooling from 873 K. Supposing that these aggregates are in the form of "randomly

distributed" dimers, one has to note that their spectroscopic characteristic (e.g. $\tau = 860$ nsec) is slightly different than in the case of dimers which form the Na_2EuCl_4 particles in the slightly doped AG-crystals ($\tau = 615$ nsec). On the other hand, the value of τ obtained in the former case is in satisfactory agreement with that given by Capelletti and Manfredi [4] who obtained $\tau = 750$ to 850 nsec for thermally induced dimers in slightly doped crystals.

For heavily doped AG crystals the luminescence decay curves become more complex, and the degree of complexity depends on λ_{em}. While for $\lambda_{em} = 410$ to 430 nm the decay curves consist of three distinguishable time-regimes (short exponential decay at the very beginning is followed by a non-exponential decay which transforms into the exponential one at the end of the process), a single exponential decay is typical for longer emission wavelengths. The lifetime value characteristic of the initial exponential decay is independent of λ_{em}, the $\alpha(e_g)$ and the testing temperature; it amounts to about 40 nsec. The origin of this behaviour can be ascribed to the supermigration of the excitation energy, [14]. The non-exponential contribution, which fits very well the Förster type exp $(-t^{1/2})$ dependence [15], is larger for crystals with the C-type absorption spectrum than for those with the D-type spectrum, is the stronger the shorter the λ_{em}, and becomes much shorter when measured at RT. The long-time exponent is distinctly dependent upon λ_{em} for the high energy side of the emission band, and remains nearly constant above 440 nm. The effect of testing temperature (LNT → RT) is to increase the effective τ value measured for all transitions along the entire emission band.

The quantitative analysis of the experimental data on the time evolution of the luminescence and their connections with the underlying microscopic energy processes will be the subject of a separate paper.

3.2. ITC data

The I–V dipole band, positioned at about 219 K, appears in the AG state spectrum only for crystals with $\alpha(e_g) \lesssim 20\,cm^{-1}$, whereby its height decreases with the increasing value of $\alpha(e_g)$. On the other hand, although the height of this band strongly increases for the solution treated samples, the calculated concentration (assuming the C_{2v} symmetry) of isolated I–V dipoles is smaller than the entire dopant concentration for $\alpha(e_g)$ as low as $20\,cm^{-1}$ [8]. In agreement with the previous statement (Section 3.1), the remaining part of the dopant is probably present in the form of small aggregates among which the dimers could be counted as the dominating ones.

As has been previously evidenced [10], the behaviour of the above-RT band, detected for all AG samples, can be understood by assuming the presence of some europium precipitate particles segregated near the dislocation lines. This corresponds very well with the behaviour of the Na_2EuCl_4 phase detected roentgenographically [1]. Hence, it is concluded that these particles should be present in practically all AG samples, in agreement with the emission data.

3.3. Precipitation strengthening effects

Fig. 5 presents the yield stress value (σ_0) of AG crystals against $\alpha(e_g)$ which represents the dopant concentration (see the comments in Section 2). Extrapolating the initial part of this plot to $\alpha(e_g) = 0$, the σ_0 value obtained ($1.5\,MNm^{-2}$) corresponds to the value characteristic of nominally pure NaCl crystals [16]. It is supposed that the effect of the dopant is simple additive to the internal friction stress characteristic of the matrix.

The increase of $\alpha(e_g)$ is accompanied by the increase of σ_0 which reaches a maximum value in a transition range of $\alpha(e_g)$. The "plateau" is typical of crystals for which the absorption spectrum corresponds to the C → D transition. The relative softening of crystals with $\alpha(e_g)$ larger than approximately $40\,cm^{-1}$ is a phenomenon typical of overaged metal alloys. Moreover, similar behaviour of a moderately doped $NaCl:Eu^{2+}$ crystal annealed at 200° C (for very long times) has been detected by Martin *et al.* [17]. It is, however to the first time that the softening appears as a "concentration-induced" phenomenon.

The mentioned similarity in the mechanical behaviour makes it possible to explain the observed strengthening phenomena in terms of the models originally elaborated for precipitation-strengthened metal alloys. Hence:

The strengthening observed for crystals with the A-, B- and C-type absorption relates with the cutting mechanism anticipated by Kelly and Nicholson [18]: the dispersed particles of a coherent (or semicoherent, at least) phase are penetrable for the moving dislocations.

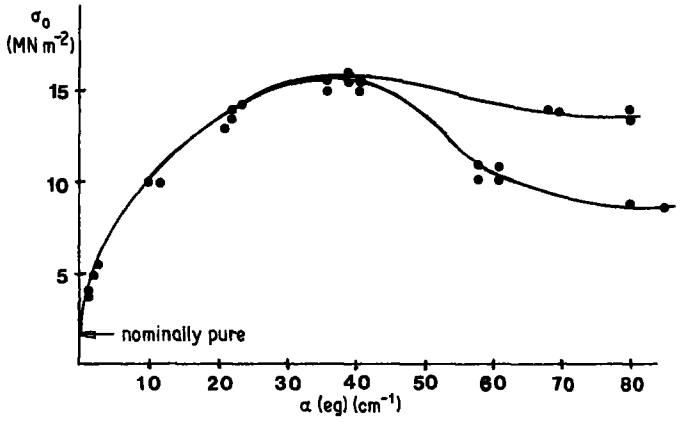

Figure 5 Dependence of the yield stress (σ_0) upon the dopant concentration, represented by $\alpha(e_g)$, for as grown crystals.

The relative softening, typical of crystals with the D-type absorption, is governed by the Orowan mechanism [19], according to which the moving dislocations bypass the unpenetrable particles (incoherent in nature) and form the Orowan loops. The two "Orowan plots", observed for approximately the same $\alpha(e_g)$, have been obtained for samples prepared from different crystal ingots. This diversity in the mechanical behaviour can be related with some differences either in the density of grown-in dislocations or in the geometry (size, shape) of the precipitate particles. It should be noted that also the emission spectra of these crystals are somewhat different, see curves (△) and (▼) of Fig. 2.

Additional confirmation of the proposed interaction mechanism was obtained from a set of data concerning the stress–strain relations. As far as the strengthened crystals exhibit the 3-stage deformation curve with the relatively low value of θ within the easy glide range, a parabolic relation, with large θ, is typical of crystals which show the relative softening. The pertinent deformation modes (monoglide in the former case and multiple glide in the latter one) correspond well with the assumed strengthening mechanisms [20].

4. Final remarks

Summarizing, we may conclude that the presence of Eu^{2+} ions introduces a variety of effects in the AG NaCl: Eu^{2+} crystals, including changes in the optical, dielectrical and mechanical properties. Despite the certain amount of obscurity left in the interpretation of some of the data, the experiments performed provided a number of details about the nature of the precipitates characteristic of various dopant concentration ranges. It has been shown that the classification of the optical absorption spectra yields a useful indication of the preferred behaviour of any AG crystal belonging to a pertinent concentration range of the dopant. Although the character of practically any type of absorption spectrum observed is likely to be determined by the sum of weighted contributions characteristic of Eu^{2+} sites in various crystallographic surroundings, the observed sequence of spectra corresponds to the following changes in the structure of precipitates: (I–V dipoles + small aggregates) → Na_2EuCl_4 → regular $EuCl_2$ of CaF_2-type → orthorhombic $EuCl_2$ of $PbCl_2$-type.

Although the majority of macroscopic data agrees well with the main features of the phases detected roentgenographically, the mechanical response of crystals in which the Na_2EuCl_4 particles should dominate cannot be understood in terms of the CsCl-type structure proposed for this phase [1]. As has been noted previously (Section 3), the strengthening due to the cutting mechanism requires the cut particles to be coherent or semicoherent, at least, with the matrix lattice. It is obvious that this requirement cannot be fulfilled by the bcc type inclusion with respect to the fcc type matrix. It should be remembered that the crystallographic analysis has been performed on the basis of only a small number of reflexes [21]. Taking into account the stoichiometry, lattice parameter value and the electroneutrality conditions, the simplest possible type of unit cell has been proposed.

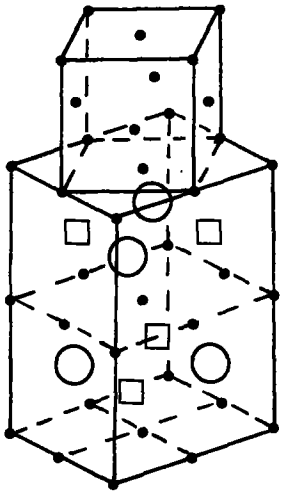

Figure 6 Model of the Na_2EuCl_4 structure: only the cationic sublattice is shown, where (●), (○) and (□) mark the Na^+ ions, Eu^{2+} ions and cation vacancies, respectively. The upper cube represents the NaCl unit cell.

In order to remove the apparent disagreement, mentioned above, we propose a model of the Na_2EuCl_4 structure which is compatible with all results obtained. Fig. 6 presents the relative orientation (one from among the possible three) of both lattices as well as the distribution of the dopant. As can be seen, the ⟨1 1 0⟩-type I–V dipoles are segregated on the {1 0 0} plane in the form of planar quadripoles, whereby two such dimers occupy the half number of cation sites within the unit cell. The dipoles within each dimer as well as the two dimers within each unit cell are arranged in a way which reduces the electrostatic constraints between the neighbouring lattice sites, [22]. It should be noted that the calculated distances between both, the base edges of the unit cell as well as between 2 Eu^{2+} ions belonging to the neighbouring dimers (along the ⟨1 1 2⟩ direction), are in reasonable agreement with the roentgenographical data. The lattice distortion amounts to about 6%, and this misfit is likely to be accommodated within the stress fields of dislocations around which the particles of the phase considered are preferentially segregated. In this way, the information of the present study along with the microstructural data provide a more complete picture of the precipitations occurring in the AG NaCl: Eu^{2+} system.

Acknowledgements

The authors are particularly grateful to Mrs T. Morawska-Kowal for preparation of the crystals. Many valuable discussions with Dr J. Stępień-Damm and assistance in performing the resolution of emission spectra by Dr R. Cywiński are also acknowledged.

References

1. J. STĘPIEŃ-DAMM and K. ŁUKASZEWICZ, *Acta Cryst* **A36** (1980) 54.
2. J. M. GARCIA, J. A. HERNANDEZ, E. H. CARILLO and J. O. RUBIO, *Phys. Rev.* **B21** (1980) 5012.
3. F. J. LOPEZ, H. S. MURRIETA, J. A. HERNANDEZ and J. O. RUBIO, *Phys. Rev.* **B22** (1980) 6428.
4. R. CAPELLETTI and M. MANFREDI, *Phys. Status Solidi (a)* **86** (1984) 333.

5. E. MUGEŃSKI and R. CYWIŃSKI, *ibid.* (*b*) **128** (1984) K75.
6. R. VOSZKA, J. TARJAN, L. BERKES and J. KRAJSOVSZKY, *Kristall u. Technik* **1** (1966) 423.
7. A. J. HERNANDEZ, W. K. CORY and J. O. RUBIO, *Jpn J. Appl. Phys.* **18** (1979) 533.
8. M. SUSZYŃSKA, H. OPYRCHAŁ, K. D. NIERZEWSKI, B. MACALIK and A. GUBAŃSKI, *Crystal Res. Technol.* **21** (1986) 931.
9. C. BUCCI, R. FIESCHI and G. GUIDI, *Phys. Rev.* **148** (1966) 816.
10. M. SUSZYŃSKA and R. CAPELLETTI, *Crystal Res. Technol.* **19** (1984) 1385, 1489.
11. *Idem, ibid.* **20** (1985) 1363.
12. M. WAGNER and W. E. BRON, *Phys. Rev.* **139** (1965) A 223.
13. J. HEBER, *Phys. Status Solidi* **42** (1970) 497.
14. A. J. BURSTEIN. *Zh. Exper. i Teoret. Fiz.* **62** (1972) 1695.
15. T. FÖRSTER, *Zs. Naturforsch.* **4a** (1949) 321.
16. M. SUSZYŃSKA, *Bull. Acad. Polon. Sci., Ser. Sci. Technol.* **25** (1977) 89.
17. J. J. MARTIN, V. J. HARNESS, E. M. OROZCO, A. A. MENDOZA and J. O. RUBIO, *Phil. Mag.* **46** (1982) 629.
18. A. KELLY and R. B. NICHOLSON, in "Progress in Material Sciences", Vol. 10, edited by B. Chalmers, (Pergamon Press, Oxford, 1963) p. 141.
19. E. OROWAN, in "Discussion in Symposium on Internal Stresses in Metals and Alloys" (Institute of Metals, London, 1948) p. 451.
20. M. F. ASHBY, in "Strengthening Methods in Crystals", edited by A. Kelly and R. B. Nicholson (Elsevier, London, 1971) p. 137.
21. J. STĘPIEŃ-DAMM, PhD thesis, Institute of Low Temperature and Structure Research, Wrocław (1980).
22. J. H. CRAWFORD Jr, *J. Phys. Chem. Solids* **31** (1970) 399.

Received 16 January
and accepted 30 June 1986